A Simple and Effective Modification of PCBM for Use as an Electron Acceptor in Efficient Bulk Heterojunction Solar Cells

ARTICLE *in* ADVANCED FUNCTIONAL MATERIALS · FEBRUARY 2011

Impact Factor: 11.81 · DOI: 10.1002/adfm.201001807

ADVANCED FUNCTIONAL MATERIALS
www.afm-journal.de

A Simple and Effective Modification of PCBM for Use as an Electron Acceptor in Efficient Bulk Heterojunction Solar Cells

John A. Mikroyannidis, Antonis N. Kabanakis, S. S. Sharma, and Ganesh D. Sharma**

[6,6]-phenyl-C-61-butyric acid methyl ester (PCBM) and poly(3-hexylthiophene) (P3HT) are the most widely used acceptor and donor materials, respectively, in polymer solar cells (PSCs). However, the low LUMO (lowest unoccupied molecular orbital) energy level of PCBM limits the open circuit voltage (V_{oc}) of the PSCs based on P3HT. Herein a simple, low-cost and effective approach of modifying PCBM and improving its absorption is reported which can be extended to all fullerene derivatives with an ester structure. In particular, PCBM is hydrolyzed to carboxylic acid and then converted to the corresponding carbonyl chloride. The latter is condensed with 4-nitro-4'-hydroxy-α-cyanostilbene to afford the modified fullerene F. It is more soluble than PCBM in common organic solvents due to the increase of the organic moiety. Both solutions and thin films of F show stronger absorption than PCBM in the range of 250–900 nm. The electrochemical properties and electronic energy levels of F and PCBM are measured by cyclic voltammetry. The LUMO energy level of F is 0.25 eV higher than that of PCBM. The PSCs based on P3HT with F as an acceptor shows a higher V_{oc} of 0.86 V and a short circuit current (J_{sc}) of 8.5 mA cm^{-2}, resulting in a power conversion efficiency (PCE) of 4.23%, while the PSC based on P3HT:PCBM shows a PCE of about 2.93% under the same conditions. The results indicate that the modified PCBM, i.e., F, is an excellent acceptor for PSC based on bulk heterojunction active layers. A maximum overall PCE of 5.25% is achieved with the PSC based on the P3HT:F blend deposited from a mixture of solvents (chloroform/acetone) and subsequent thermal annealing at 120 °C.

1. Introduction

Polymer solar cells (PSCs) have emerged as a promising alternative technique for producing clean and renewable energy due to their potential for fabrication onto large areas of lightweight flexible substrates by low-cost solution processing. To maximize the donor-acceptor heterojunction interfacial area for efficient exciton dissociation, mainstream PSC devices adopt the concept of a bulk heterojunction (BHJ), where an active layer contains a p-type donor and an n-type acceptor to form an interpenetrating nanoscale network.[1] A conventional BHJ PSC with an active layer sandwiched by a low-work-function aluminum cathode and a hole-conducting poly(3,4-ethylenedioxylenethiophene):poly(styrenesulfonic acid) (PEDOT:PSS) layer on top of an indium tin oxide (ITO) substrate is the most widely used and investigated device configuration. Broad visible–NIR absorption, higher charge carrier mobility, and suitable electronic energy levels of both the donor and acceptor materials are crucial for high-efficiency PSCs.[2] Poly(3-hexylthiophene) (P3HT) is the most representative conjugated polymer donor material, and [6,6]-phenyl-C-61-butyric acid methyl ester (PCBM) is the most important acceptor material. Power conversion efficiency (PCE) of 4–5% has been reached for the PSCs based on the P3HT/PCBM system by device optimization.[3–5] In order to further improve the PCE of the PSCs, much research work has been devoted to finding new conjugated polymer donor materials aiming at broader absorption, lower band gap, higher hole mobility, and

Prof. J. A. Mikroyannidis, A. N. Kabanakis
Chemical Technology Laboratory
Department of Chemistry
University of Patras
GR-26500 Patras, Greece
E-mail: mikroyan@chemistry.upatras.gr
Prof. G. D. Sharma
Physics Department
Molecular Electronic and Optoelectronic Device Laboratory
JNV University
Jodhpur (Raj.) 342005, India
Email: sharma_in@yahoo.com
Prof. G. D. Sharma
R & D Centre for Engineering and Scicence
Jaipur Engineering College
Kukas, Jaipur (Raj.), India
S. S. Sharma
Department of Physics
Government Engineering College for Women
Ajmer, Rajasthan, India
S. S. Sharma
Thin Film and Membrane Science Laboratory
University of Rajasthan
Jaipur, Rajasthan, India

DOI: 10.1002/adfm.201001807

suitable electronic energy levels, and some donor–acceptor (D–A) copolymers show higher photovoltaic (PV) efficiency than P3HT. Nevertheless, the research efforts toward new C_{60} derivative acceptor materials to replace PCBM have not been very successful until now.

PCBM has been prepared by Hummelen and Wudl in 1995.[6] It offers the advantages of good solubility in organic solvents such as chloroform, chlorobenzene, dichlorobenzene, etc., higher electron mobility, and higher electron affinity.[1a,1e,3–5,7] However, weak absorption in the visible region and a low LUMO energy level are its weak points. Weak absorption in the visible region limits its contribution to light harvesting in the PV conversion. The low LUMO energy level of the acceptor material results in lower open circuit voltage (V_{oc}) of the PSCs, since the V_{oc} of the PSCs is proportional to the difference between the LUMO energy level of the acceptor and the HOMO energy level of the donor.[8] Therefore, it is very important to design and synthesize new soluble fullerene derivatives with stronger visible absorption and higher LUMO energy levels than PCBM. Although many C_{60} derivatives[9–16] and a new C_{84} derivative[17] have been synthesized and used as acceptors in PSCs, most of the device performance is poorer than or similar to that of PCBM. [6,6]-phenyl-C-71-butyric acid methyl ester ($PC_{70}BM$), which has a broader absorption in the visible region than PCBM, shows improved PV performance over PCBM,[18–22] PCBM bis-adduct (bisPCBM) shows ca. 0.1 eV higher LUMO energy level than PCBM, and the PCE of the PSC based on P3HT and bis-PCBM reached 4.5%, an increase of 18% over that of PCBM, which results from a higher V_{oc} of 0.73 V owing to the higher LUMO energy level of the acceptor.[23] Recently, a novel endohedral fullerene, $Lu_3N@C_{80}$-PCBH, has been reported, which also possesses a higher LUMO energy level than PCBM.[24] The P3HT-based PSCs with $Lu_3N@C_{80}$-PCBH as acceptor showed higher V_{oc} (0.26 V higher) than the device with PCBM as acceptor. Nevertheless, the high cost of $PC_{70}BM$ and $Lu_3N@C_{80}$-PCBH can limit their future commercial application in PSCs. A remarkable bis-adduct fullerene derivative, ICBA, formed by two indene units covalently connected to the fullerene sphere of C_{60} has recently been reported by Hou and Li.[25] Interestingly, the presence of two aryl groups improves the visible absorption compared to the parent PCBM, as well as its solubility (>90 mg mL^{-1} in chloroform) and the LUMO energy level, which is 0.17 eV higher than PCBM. The PV devices formed with P3HT as the semiconducting polymer revealed PCE values of 5.44% under illumination of AM1.5, 100 mW cm^{-2}, thus surpassing PCBM which afforded an efficiency of 3.88% under the same experimental conditions. More recently, device optimization of BHJ PSCs based on P3HT as donor and ICBA as acceptor has been performed by the same research group. In particular, the optimized PSC with the P3HT:ICBA weight ratio of 1:1, solvent annealing and pre-thermal annealing at 150 °C for 10 min, has exhibited a high PCE of 6.48% with V_{oc} of 0.84 V, J_{sc} of 10.61 mA cm^{-2}, and FF of 72.7%, under the illumination of AM 1.5G, 100 mW cm^{-2}. These values are the highest reported in the literatures so far for P3HT based PSCs.[26]

A major drawback in the synthesis of bis-adducts of fullerenes is that the products formed consist of a mixture of regioisomers which are not separated because of the experimental difficulties. Chemically modified fullerenes for BHJ solar cells have been recently reviewed.[27] The synthesis of new fullerene derivatives with stronger visible absorption and higher LUMO energy levels than PCBM is currently a challenge for all those chemists engaged in the chemical modification of fullerenes for PV applications.

In the present investigation we report a simple synthesis of a modified fullerene derivative, **F**, in three steps. It included the hydrolysis of PCBM to carboxylic acid, which was subsequently converted to the corresponding carbonyl chloride. Finally, the latter reacted with 4-nitro-4'-hydroxy-α-cyanostilbene (NHCS) to afford **F**. NHCS is a low cost product which has been prepared in our laboratory from one-step reaction from inexpensive and widely used starting materials. Details for the synthesis, characterization and utilization of NHCS in dye-sensitized solar cells have been reported in our previous publication.[28] The modified fullerene **F** possesses the ester structure like PCBM. However, the ester methyl group of PCBM has been replaced in **F** by the large 4-nitro-α-cyanostilbene moiety. This replacement aimed to increase the absorption, enhance the solubility and suppress the crystallization. Interestingly, **F** shows higher solubility in common organic solvents and stronger absorption than PCBM in the range of 250–900 nm. It is worth noticing that the present modification process can be readily applied to all fullerene derivatives bearing the ester structure, such as $PC_{70}BM$, ThCBM (which contains thiophenyl instead of phenyl) and PCBM- or ThCBM-bisadducts. The LUMO energy level of **F** is 0.25 eV higher than that of PCBM. The PSC based on the P3HT with **F** as electron acceptor displayed higher V_{oc} of 0.86 V and a PCE of 4.23%, when the blend was cast from chloroform solvent, while the device based on P3HT:PCBM displays PCE of 2.93% under the same conditions. This indicates that **F** is superior to PCBM when it is used as electron acceptor along with conjugated polymers as electron donor in PSCs. We have also fabricated PSCs with the BHJ active layer (P3HT:**F**) deposited from a mixture of solvents (chloroform/acetone) and subsequent thermal annealing and achieved PCE of 4.62% and 5.25%, respectively. The higher PCE for the device with the BHJ deposited from the mixture of solvents and further improvement with subsequent thermal annealing has been attributed to the increase in the crystallinity of the P3HT. The interpenetrating network structure forms the in situ self organized P3HT crystallites in the BHJ and produces controlled bi-continuous percolation pathways that enhance both hole and electron mobilities, affording higher photocurrent.

2. Results and Discussion

2.1. Synthesis and Characterization

The synthetic route to modify PCBM is shown in **Scheme 1**. Starting from PCBM, the carboxylic acid (PCBA) was obtained by treatment with hydrochloric acid and acetic acid in toluene.[29] It was further reacted with thionyl chloride in CS_2 solution to form the corresponding carbonyl chloride (PCBC).[29] The latter reacted with an equivalent amount of NHCS[28] in pyridine to afford the target **F** as a greenish-brown solid in 82% yield. In this reaction, pyridine acted as both reaction medium and acid scavenger. The reaction product was repeatedly washed with

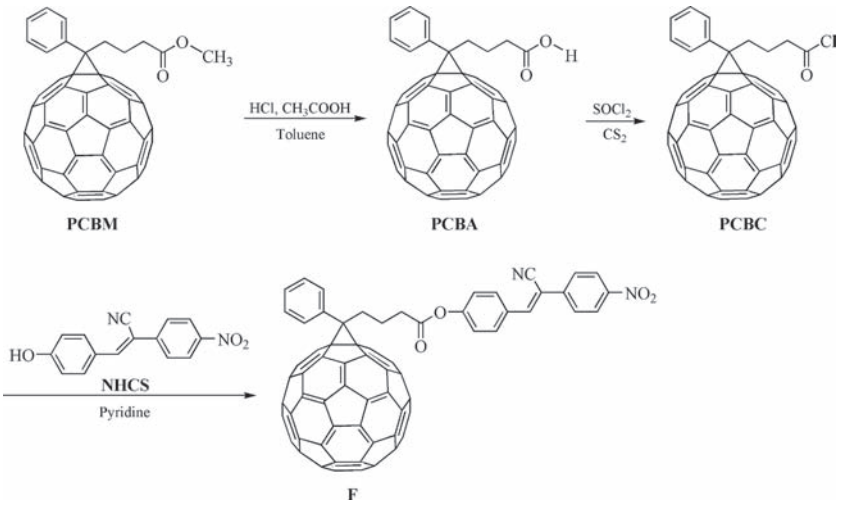

Scheme 1. Synthesis of **F**.

methanol to dissolve any possible un-reactive NHCS and finally purified by silica column chromatography. Since the organic moiety of **F** was increased by this modification, the modified fullerene displayed higher solubility than PCBM in common organic solvents, such as chloroform and tetrahydrofuran (THF)(≈40 mg mL^{-1}). The solubility of PCBM in these solvents is ≈25 mg mL^{-1}.

Structural characterization of **F** was accomplished by Fourier-transform infrared (FTIR) and ^{1}H NMR spectroscopy. **Figure 1** presents the IR spectra of PCBM and **F**. Both spectra showed absorption bands around 523, 574, 1182, and 1426 cm^{-1} associated with the fullerene. Besides, **F** displayed characteristic absorptions at 2200 (cyano) and 1516, 1340 cm^{-1} (nitro). In addition, the carbonyl stretching vibration of the ester shifted from 1736 cm^{-1} in PCBM to 1702 cm^{-1} in **F**. On the other hand

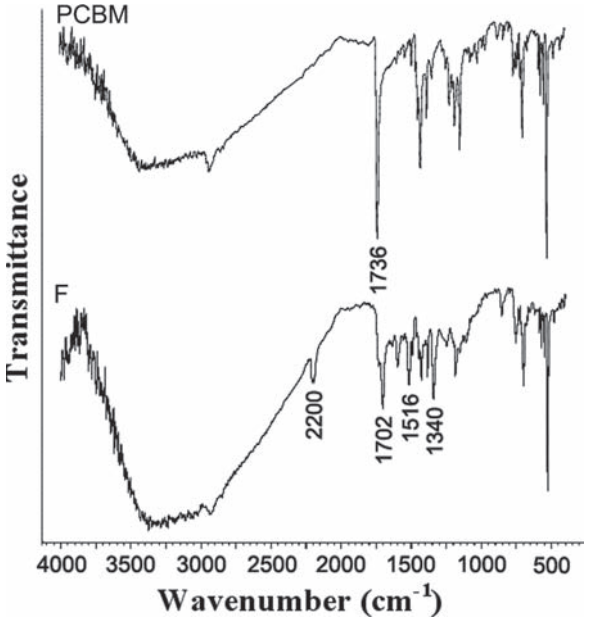

Figure 1. FTIR spectra of PCBM (top) and **F** (bottom).

in the ^{1}H NMR spectrum of **F**, the signals of the aliphatic segments remained the same with those of PCBM. However, the resonances of **F** assigned to the aromatic were significantly differentiated from the corresponding of PCBM. In particular, **F** showed an upfield signal at 8.17 ppm assigned to the phenylene ortho to nitro. The other aromatic of **F** as well as the cyanovinylene resonated at the region of 7.84–7.06 ppm. These changes in the IR and ^{1}H NMR spectra supported the successful modification of PCBM.

2.2. Photophysical Properties

For PV applications the absorption, especially in the visible region, is a significant property. For this reason, $PC_{70}BM$ is superior to PCBM, when it is used as electron acceptor in PV devices. The absorption of **F** was investigated in both dilute (10^{-5} M) chloroform solution and thin film. The thin film was prepared from chloroform solution of **F** by spin coating on quartz substrate. **Figure 2** shows the UV–vis absorption spectra of PCBM and **F** in chloroform solution for the spectrum range of 250–900 nm (top) and 400–800 nm (bottom). The small peak

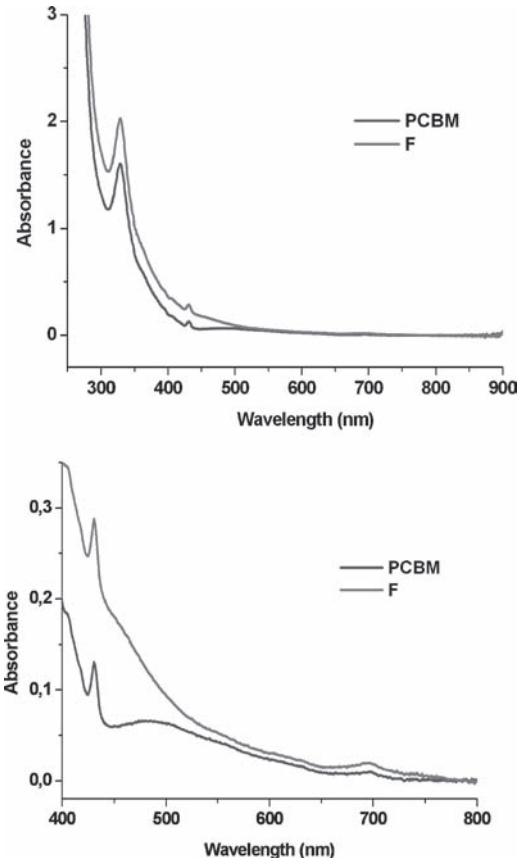

Figure 2. UV–vis absorption spectra of PCBM and **F** in chloroform solution for the spectrum range of 250–900 nm (top) and 400–800 nm (bottom).

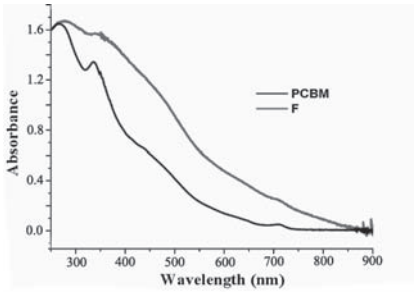

Figure 3. UV–vis absorption spectra of PCBM and **F** in thin film.

approximately at 700 nm is assigned to the [6,6]-addition in C_{60}. It can be seen from these figure that the absorption of **F** is stronger than that of PCBM in all spectrum region. It should be noted that certain modified fullerenes, such as an indene-C_{60} bis-adduct,[25] had displayed in solution stronger absorption than PCBM only in the visible region (400–800 nm), while it was weaker in the UV region (below 300 nm). Interestingly, the thin film absorption of **F** was also much stronger than that of PCBM in all spectrum region (**Figure 3**). The thin film absorption coefficient ranged from 5.3×10^4 M^{-1} cm^{-1} to 2.5×10^4 M^{-1} cm^{-1} for **F** and from 2.4×10^4 M^{-1} cm^{-1} to $1.2 \times 10^4 M^{-1}$ cm^{-1} for PCBM, for the wavelength region of 380–500 nm. These results support that **F** is a better electron acceptor than PCBM from the viewpoint of light absorption.

2.3. Electrochemical Properties PCBM and F

Electrochemistry is one of the most important properties of fullerene derivatives.[30] Therefore, we studied the electrochemical properties of PCBM and **F** by CV (**Figure 4**). The LUMO levels of PCBM and **F** were estimated from their onset reduction potentials indicated in cyclic voltammograms.[31] The onset reduction potentials (E_{red}) of PCBM and **F** were –0.75 V and –0.95 V versus Ag/Ag^+, respectively. From the onset reduction potentials, the LUMO energy levels of PCBM and **F** were calculated according to the equation:[32] LUMO = –q (E_{red} + 4.7), where q is electronic charge and E_{red} is the onset reduction potential (in V) versus Ag/Ag^+. The LUMO levels of PCBM and **F** estimated from the cyclic voltammogram are –3.95 eV and –3.75 eV, respectively. The LUMO level of **F** is raised by 0.20 eV in comparison with that of PCBM. This shift is attributed to the presence of the strong electron withdrawing nitro and cyano groups in the molecule of **F**, which increase its electron affinity (acceptor strength), thus leading to higher shift value than that reported for PCBM bis-adduct (bisPCBM).[24] The higher LUMO energy level of **F** is desirable for its application as acceptor in polymer BHJ PV devices to get higher voltage.

The onset oxidation potentials (E_{ox}) for PCBM and **F** are 1.5 V and 1.2 V versus Ag/Ag^+, respectively. This indicates that the onset oxidation potential for **F** shifts by –0.3 V as compared to PCBM. The HOMO energy levels of PCBM and **F** were estimated from their onset oxidation potentials, which were obtained from the cyclic voltammograms of Figure 4. From the onset oxidation potentials, the HOMO energy levels of PCBM and **F** were calculated according to the equation:[32] HOMO = –q (E_{ox} + 4.7), where E_{ox} is the onset oxidation potential (in V) versus Ag/Ag^+. The HOMO energy levels of PCBM and **F** calculated from cyclic voltammogram are –6.2 eV and –5.9 eV, respectively. The results indicate that the HOMO energy level of **F** shifted upwards in comparison to that of PCBM.

2.4. Optical Properties of Blends

The absorption spectra of P3HT:PCBM and P3HT:**F** thin films deposited from chloroform solution are shown in **Figure 5**a. It can be seen from this figure that the absorption spectra of the blends show the combination of individual components. The absorption peak around 525 nm corresponds to the P3HT component, which is associated with interchain π to π^* transition.[33] The absorption shoulder at around 615 nm is related to the interchain interaction and the height of this shoulder indicates the ordering of the chain packing.[33,34] The optical absorption spectra of the P3HT:**F** blend show broader band as compared to P3HT:PCBM, which is attributed to the absorption of **F** in the lower wavelength region. Upon the addition of acetone to the blend solution in chloroform, the absorption band is red shifted and the intensity is increased (Figure 5b). A further red shift in the absorption band has also been observed for thermally annealed blends. A high degree of P3HT crystallinity was indicated by a red shift in the absorption band, clear vibronic shoulder appeared at long wavelengths (between 610 and 625 nm) as the enhanced interchain π–π^* stacking, and increased absorption intensity. During the spin coating process, the blend solutions with ordered precursors solidified into film structures as the majority of solvent evaporated from the blend solution. The blend film from the mixed solvents showed higher

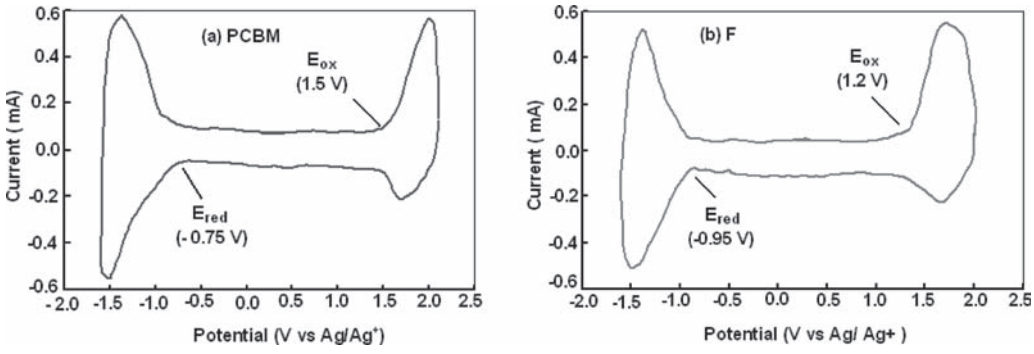

Figure 4. Cyclic voltammograms of a) PCBM and b) **F** at scan rate 100 mV s^{-1}.

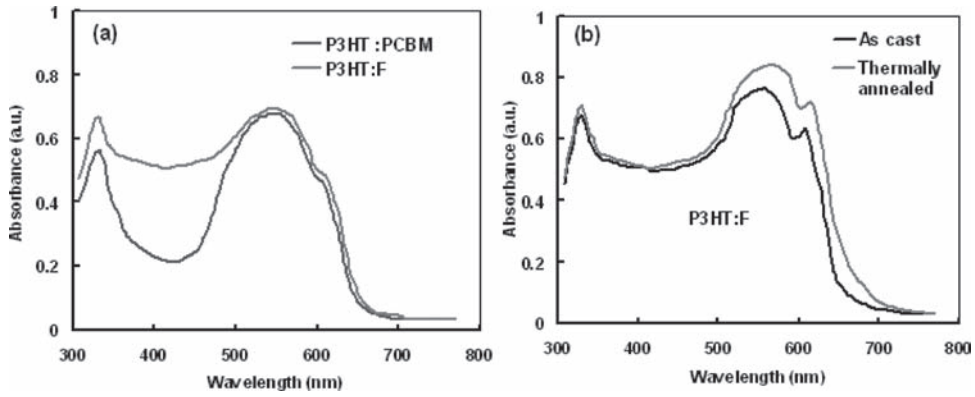

Figure 5. Absorption spectra of a) P3HT:PCBM (1:1 w/w) and P3HT:**F** (1:1 w/w) blends in thin films deposited from chloroform solution; b) as-cast and subsequent thermally annealed P3HT:**F** blend film deposited from mixed solvents.

crystallinity than the film cast from a good solvent. Figure 5b clearly shows that the crystallinity of the blend film was enhanced by thermal annealing. Thermal annealing treatment allowed the film to crystallize more extensively, as indicated by the increased absorption intensity and the prominent vibronic features. The improved P3HT crystallinity, which is facilitated through self organized chain stacking, can enhance not only the hole transport but also the light harvesting capabilities, thus improving the photocurrent in the PV device.[35]

2.5. Photovoltaic Properties of P3HT:PCBM and P3HT:F

PCBM and modified PCBM, i.e., **F**, were used as acceptors to fabricate BHJ PSCs with P3HT as donor, and the weight ratio of the donor to acceptor was 1:1. The current–voltage (*J*–*V*) characteristics of the ITO/PEDOT:PSS/P3HT:PCBM or **F**/Al devices under illumination intensity of 100 mW cm^{-2} are shown in **Figure 6**a. The PV parameters, i.e., short circuit current (J_{sc}), open circuit voltage (V_{oc}), fill factor (*FF*) and PCE of the devices are listed in the **Table 1**. It can be seen from this table that the V_{oc} is increased from 0.68 V for PCBM-based device to 0.86 V for the **F**-based device. The higher value of V_{oc} for the PSC device based on P3HT:**F** is attributed to the higher LUMO energy level of **F**, because it is well known that the V_{oc} of PSCs is proportional to the difference between the HOMO of the donor (P3HT) and the LUMO of the acceptor.[36] The increase in the J_{sc} for the device based on P3HT:**F** in comparison to P3HT:PCBM is attributed to the broader absorption of the P3HT:**F** blend, which causes an enhancement on the photogenerated excitons in the blend, resulting slightly higher photocurrent.

The values of incident photon to current efficiency (IPCE) have been estimated using following expression

$$IPCE(\%) = 1240 J_{sc}/\lambda P_{in}$$

where P_{in} (W m^{-2}) and λ (nm) are the illumination intensity and wavelength of the monochromatic light, respectively. The IPCE spectra of the devices based on the blends are shown in Figure 6b. It can be seen from this figure that the IPCE spectra of the devices resemble the absorption spectra of the blend used in the device, indicating both components used in the blend contribute to the photocurrent. It is noted that the IPCE in the wavelength region 340–500 nm is higher for the device based on P3HT:**F** than that for P3HT:PCBM which could be ascribed to the contribution of the absorption of **F** in this wavelength

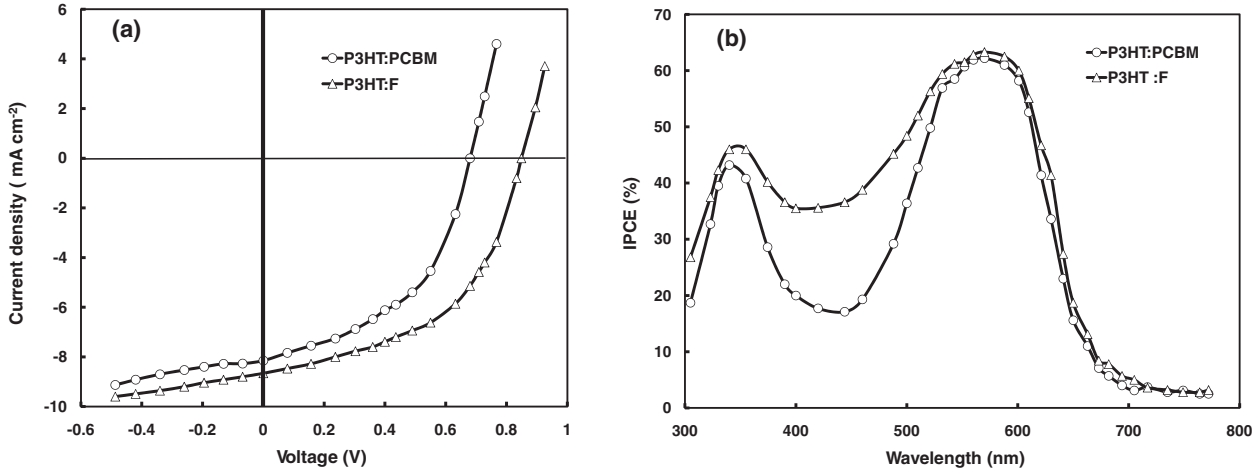

Figure 6. a) Current–voltage characteristics and b) IPCE spectra of the PSCs based on P3HT as donor and PCBM or **F** as acceptor with weight ratio 1:1 deposited from chloroform solvent.

Table 1. Photovoltaic parameters of the devices based on P3HT:PCBM and P3HT:**F** under illumination intensity of 100 mW cm^{-2}, white light.

Active layer	Short circuit current (J_{sc}) [mA cm^{-2}]	Open circuit voltage (V_{oc}) [V]	Fill factor (*FF*)	Power conversion efficiency (PCE) [%]
P3HT:PCBM[a)]	8.0	0.68	0.54	2.93
P3HT:**F**[a)]	8.5	0.86	0.58	4.23
P3HT:**F**[b)]	9.4	0.82	0.60	4.62
P3HT:**F**[c)]	10.3	0.81	0.63	5.25

a) cast from chloroform b) cast from chloroform/acetone c) cast from chloroform/acetone and subsequent thermal annealing at 120 °C.

region. The IPCE results indicate that the **F** acceptor is beneficial to the solar light harvest and affords higher photocurrent.

The solvent annealing and thermal annealing is very important for the PSCs based on the P3HT:**F** blend. The annealing process controls the morphology of the active layer and enhances the electron and hole mobilities. In most of the organic solar cells based on BHJ active layers, the electron mobility is higher than the hole mobility, which increases the recombination loss of the charge carriers.[35] Furthermore, the nanoscale morphology can deteriorate if the acceptor (PCBM) domains grow beyond the length scale of exciton diffusion, thereby prohibiting efficient charge transfer.[37] Thermal annealing at relatively high temperature also has risks, such as oxidation and degradation of the active layer used in the device.[38] In addition to thermal annealing, solvent annealing can improve the nanoscale morphology of the BHJ layer by promoting polymer self organization via control over the evaporation rate of the residual solvent.[3,39] Aside from the thermal and solvent annealing processes, annealing free approaches have been also developed. P3HT nano-fiber formation has been promoted through the cooling of a saturated P3HT solution.[40] Mixed solvents approaches allow control over the active layer morphologies in blend films.[41] However, it is difficult to obtain optimized morphologies of blend films through the above mentioned treatments, because polymer (donor) crystallization and phase separation of the two components occur within a single step, and the two processes can, therefore, interfere with each other. It is difficult to effectively control both polymer (donor) crystallization and acceptor diffusion to ensure the presence of bi-continuous pathways for charge carriers and an appropriate interface area.[41b] We have prepared BHJ active layer, formed from a two-step process, consisting first of the crystallization of P3HT, through the addition of the marginal solvent, i.e., acetone, to the blend solution in chloroform, followed by the nanoscale phase separation achieved through thermal annealing at 120 °C. The PSCs were fabricated using P3HT:**F** active layer spin cast from the mixed solvents having structure ITO/PEDOT:PSS/P3HT:**F**/Al. Since **F** is a modified form of PCBM, this concept may also be feasible for P3HT:PCBM blend. The performance and the characteristics of these devices, with the additional thermal annealing step, were measured and compared. The *J–V* characteristics and the corresponding incident photon to current efficiency (IPCE) are shown in **Figure 7**a and b, respectively. The PV parameters for the devices are summarized in Table 1. For the device based on mixed solvents without thermal annealing, the performance reached a PCE of 4.75%. Upon thermal annealing at 120 °C, the device PCE has been enhanced up to 5.25%. The IPCE spectra of the devices (Figure 7b) also confirmed the increase in the J_{sc} as indicated by the magnitude and broad shape of the IPCE spectra. The IPCE spectral curve of the device fabricated from the mixed solvents display broader band region than the device formed from the single solvent. The value of IPCE has been further increased when the device was fabricated with the thermally annealed blend. The red shift of the IPCE spectra, which agreed well with the red shift observed in the absorption spectra of the blend films, was interpreted as arising from the enhanced P3HT crystallinity and resulting improved hole mobility. The enhancement in the value of IPCE and PCE of devices based on mixed solvents and additional thermal annealing is mainly due to the increase in the J_{sc} photocurrent.

A drop in V_{oc} occurred for the device fabricated with mixed solvents and also with an additional thermal annealing. It is widely accepted that the V_{oc} for organic BHJ solar cells is determined by the energy difference between the HOMO level of donor and the

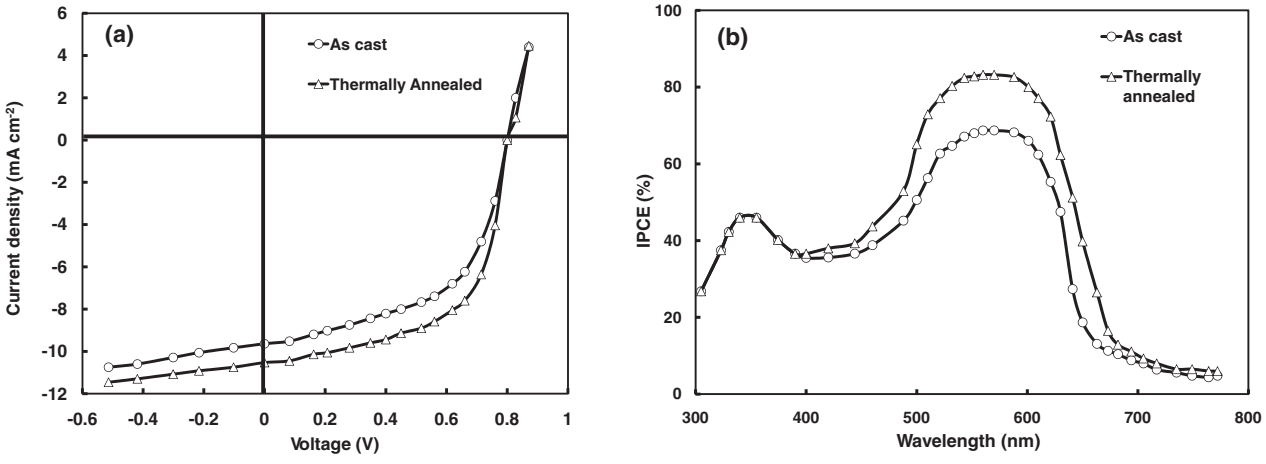

Figure 7. a) *J–V* characteristics under illumination and b) IPCE spectra of the devices based on the as-cast and thermally annealed P3HT:**F** blend films deposited from mixed solvents.

LUMO level of acceptor.[42] It can be seen from the absorption spectra of the P3HT:**F** blend deposited from the mixed solvent and additional thermal annealing that the onset absorption edge shifted towards the longer wavelength region, indicating reduction in the optical band gap of P3HT. Therefore, we assume that the reduction in the band gap of P3HT, results in an upward shift in the HOMO level of P3HT, due to the extension of conjugation length and the interchain overlap,[43] as indicated in the absorption spectra of the P3HT:**F** blend. Therefore, the devices containing the P3HT:**F** blend films with higher crystallinity resulting from the mixed solvents and thermal annealing, showed lower V_{oc} than the devices with films which have lower crystallinity.

The crystallinity of the blend films was also evaluated by X-ray diffraction (XRD) measurements on the spin coated blend films. **Figure 8** shows the XRD patterns of the P3HT:**F** blend films prepared under different conditions (i.e., as-cast from chloroform, as-cast from mixed solvents and additional thermal treatment of film deposited from mixed solvents). It can be seen from this figure that the P3HT:**F** blend film fabricated from chloroform shows a diffraction peak around $2\theta = 5.8°$ which corresponds to the P3HT. When the film was deposited from the mixed solvents, the height of diffraction peak observed around $2\theta = 5.8°$ is increased and it is further increased when the film is thermally annealed. The observed increase in the intensity of diffraction peak also suggests an increase of the P3HT crystallinity, when the film was deposited from mixed solvents and additional thermal annealing. The structure of P3HT in the blend films deposited from mixed solvents included crystalline nanowires, nanocrystals and amorphous regions.[44] In the absence of thermal annealing P3HT and **F** were homogeneously mixed. During the thermal annealing process, **F** diffused and aggregated to form de-mixed domains, which organized the percolation pathways for electron transport. We assume that the blend film deposited from the mixed solvents and subsequent thermal annealing permitted fine tuning of morphology of the interpenetrating nanowire, with evenly distributed **F** domains, for the formation of bi-continuous percolation pathways and a large D–A interface area between the P3HT and **F** components. This leads to an enhancement in the photocurrent and results in higher PCE.

We have also investigated the morphologies of P3HT:**F** film cast in different conditions, i.e., cast from chloroform, chloroform/acetone and chloroform/acetone and subsequent thermal annealing at 120 °C, to get information about the average surface roughness of the film, using atomic force microscopy (AFM). The AFM images of the films cast under different conditions are shown in **Figure 9**. The average surface roughness of the

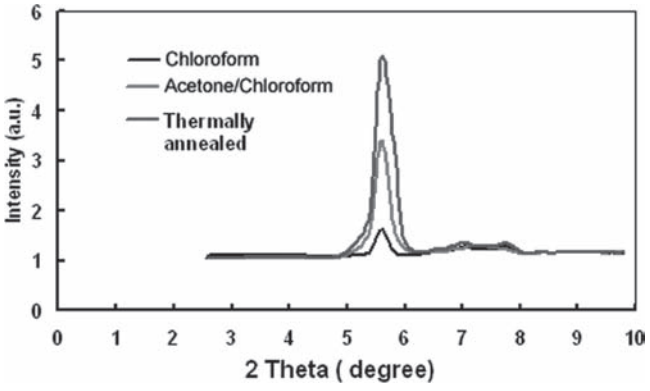

Figure 8. XRD patterns of P3HT:**F** blend films cast from chloroform, chloroform/acetone and thermally annealed at 120 °C.

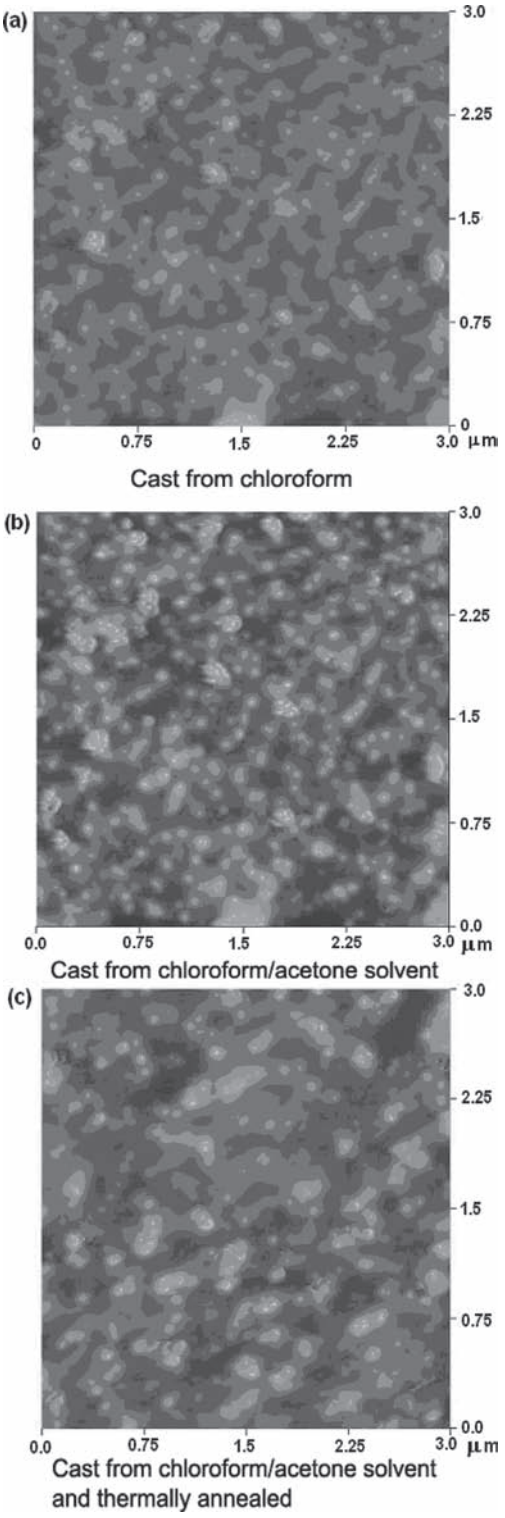

Figure 9. AFM images of P3HT:**F** blends as-cast in different conditions (3 µm × 3 µm).

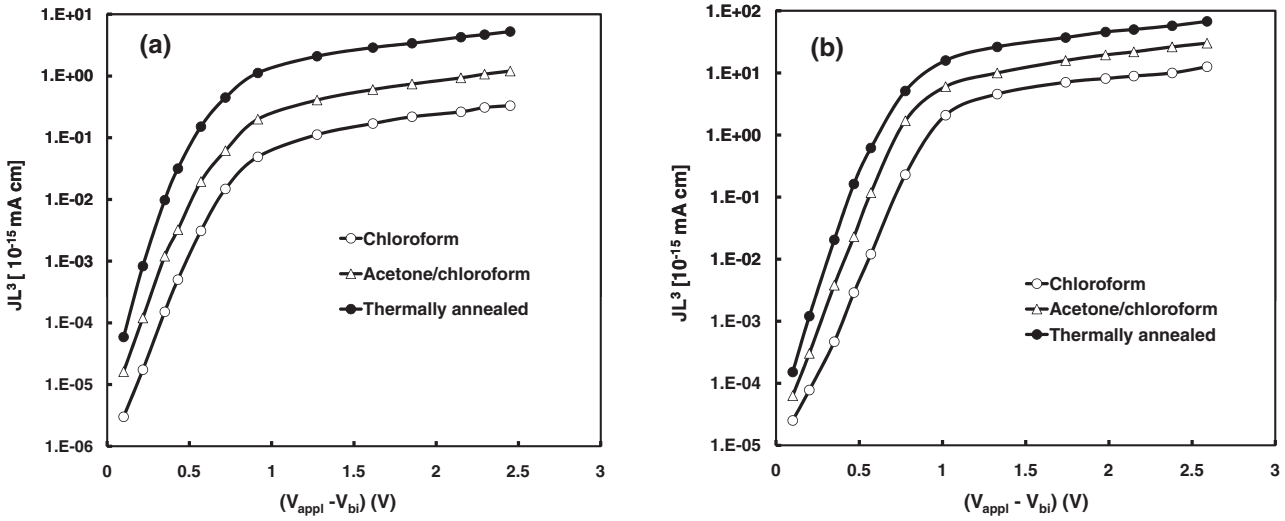

Figure 10. Current–voltage characteristics of the a) hole-only b) electron-only devices fabricated with P3HT:**F** active layers from chloroform solvent, chlorofrm/acetone solvent, and subsequent thermal annealing, where J is the current density (mA cm^{-2}) and L is the thickness of the active layer (cm).

blend films are 1.2 nm and 1.87 nm for the blend cast from the chloroform and chloroform/acetone solvent, respectively. The average surface roughness further increases to 2.6 nm, when the P3HT:**F** blend cast from the chloroform/acetone solvent is thermally annealed at 120 °C. The surface domain size has also been increased upon thermal annealing. This indicates that both increased domain size and average surface roughness results in an improvement in the crystallinity of the blend. This is responsible for the enhancement in the PCE due to the more efficient photoinduced charge transfer at the D–A interfaces and the more balanced charge transport.

For the efficient polymer BHJ solar cells, the mobility of electrons and holes in the polymer blends is an important parameter that must be well controlled because a balanced charge carrier transport is an essential prerequisite for increasing PCE and *FF*.[35,45] The space charge limited current (SCLC) method was employed to estimate the hole and electron mobilities of the devices prepared with various thin film active layers.[45] SCLC *J*–*V* characteristics were obtained in dark from the hole only devices (ITO/PEDOT:PSS/P3HT:**F**/Au) and the electron only devices (Al/P3HT:**F**/Al) as a function of the applied bias voltage, which was corrected for the built in potential $V = V_{appl} - V_{bi}$ and shown in **Figure 10**. The hole and electron mobilities were estimated from the *J*–*V* characteristics at low voltage region, where the current is described by the Mott–Gurnay square law: $J_{SCLC} = (9/8)\varepsilon_o\varepsilon_r\mu(V^2/L^3)$, where $\varepsilon_o\varepsilon_r$ is the permittivity of the polymer, μ is the charge carrier mobility, and L is the film thickness. The hole and electron mobilities of P3HT:**F** blend films cast from chloroform only, mixed solvents and subjected to thermal annealing are listed in **Table 2**. The highly ordered π–π* conjugation crystalline nature of the blend as observed in the optical absorption spectra and XRD pattern, respectively, is known to improve the charge carrier mobility in the blend films.[3,35,46] It can be seen from Table 2 that both electron and hole mobilities for the blend cast from mixed solvents is higher than that for cast from the chloroform only. When the blend film is deposited from mixed solvents, the hole mobility has been increased to 6.4×10^{-4} cm^2 V^{-1} s^{-1}, two orders of magnitude higher than the mobility of 9.6×10^{-6} cm^2 V^{-1} s^{-1} in the blend film cast from chloroform solvent, and one order of magnitude higher than the mobility measured in the film cast from chloroform only subjected to thermal annealing, which showed a mobility of 6.7×10^{-5} cm^2 V^{-1} s^{-1}. The increase in the hole mobility is attributed to the crystalline nature of the blend as indicated from the XRD data. The electron mobility was also enhanced by a factor of twenty, i.e., 3.5×10^{-5} cm^2 V^{-1} s^{-1} and 7.4×10^{-4} cm^2 V^{-1} s^{-1} for the blend cast from chloroform solvent and chloroform/acetone solvent, respectively. The electron mobility has been slightly improved when the blend deposited from chloroform/acetone solvent was subsequently thermally annealed at 120 °C. The ratio between the electron and hole mobilities approached towards unity, i.e., 1.15 and 0.94 for blend deposited from chloroform/acetone solvent and subsequent thermal annealing, respectively, resulting in highly balanced charge transport in the BHJ PV devices based on these blends. A well controlled morphology, through the enhancement in the crystallinity of P3HT, led to balance charge transport in the active blend layer, and enhanced J_{sc} and *FF*. The hole mobility in the device fabricated from chloroform solvent was insufficient to ensure efficient charge transport and the

Table 2. Electron and hole mobilities of P3HT:**F** blend films cast under different conditions, estimated using the Mott-Gurney law.

	μ_e [cm^2 V^{-1} s^{-1}]	μ_h [cm^2 V^{-1} s^{-1})	μ_e/μ_h
Cast from chloroform	3.5×10^{-5}	9.6×10^{-6}	3.64
Cast from chloroform/acetone	7.4×10^{-4}	6.4×10^{-4}	1.15
Cast from chloroform/ acetone and subsequent thermal annealing at 120 °C	1.13×10^{-3}	1.2×10^{-3}	0.94

hole and electron mobilities were less balanced than those measured for the films as-cast from chloroform/acetone solvent and subsequent thermal annealing.

3. Conclusions

Starting from PCBM, a new C_{60} derivative was successfully synthesized by a reaction of three steps. **F** showed higher solubility than PCBM being readily soluble in common organic solvents. Both solutions and thin films of **F** displayed stronger absorption than PCBM in the region of 250–900 nm. We have fabricated PSCs with the P3HT:**F** blend and compared the PV performance with that of the device based on P3HT:PCBM blend. The V_{oc} and PCE of the P3HT based PSC with **F** as electron acceptor cast from chloroform solvent, reached 0.86 V and 4.23%, respectively, under the illumination intensity of 100 mW cm^{-2}, which is significantly improved as compared to the V_{oc} of 0.68 V and PCE of 2.93% of the device with PCBM as electron acceptor under the same experimental conditions. The increase in the V_{oc} has been attributed to the higher LUMO level for **F** relative to PCBM. The J_{sc} has also been improved up to 8.5 mA cm^{-2} for the device based on **F** as compared to PCBM, which is 8.0 mA cm^{-2}, ascribed to the light absorption by the **F** in visible region.

We have also investigated the effect of mixed solvents and subsequent thermal annealing on the PV performance of the PSCs based on P3HT:**F** blend. The PCE of the PSCs based on P3HT:**F** blend deposited from acetone/chloroform solvent and subsequent thermal annealing is 4.62% and 5.25%, respectively. This increase in the PCE has been attributed to the improved P3HT crystallinity and nanoscale morphology, resulting in balanced charge transport in the blend due to the increase in both electron and hole mobilities. These results indicate that the modified PCBM, i.e., **F** is an excellent electron acceptor for PSCs and could be a promising acceptor instead of PCBM for further improving the PCE of the high performance PSCs based on low band gap conjugated polymer or small molecule donor by increasing both V_{oc} and J_{sc}.

4. Experimental Section

Reagents and Solvents: 4-nitro-4'-hydroxy-α-cyanostilbene (NHCS) has been synthesized as a dark green solid in 60% yield from the reaction of 4-hydroxybenzaldehyde with 4-nitrobenzylcyanide (mol ratio 1:1) in ethanol in the presence of sodium hydroxide.[28] PCBM was purchased from Aldrich.

*Synthesis of **F***: A flask was charged with a solution of PCBC (0.0892 g, 0.0974 mmol) in pyridine (15 mL). NHCS (0.0259 g, 0.0974 mmol) dissolved in pyridine (10 mL) was added portionwise to the stirred solution at 0 °C. The mixture was stirred and heated at 80 °C for 2 h under N_2. It was subsequently concentrated under reduced pressure and methanol was added to the concentrate and the obtained suspension was centrifuged to isolate **F**. The addition of methanol to the solid isolated and centrifugation of the resulting suspension was repeated two times. The crude reaction product was purified by silica gel column chromatography eluting with toluene/THF (1:1) to afford **F** as a greenish-brown solid (0.0914 g, 82%). FTIR (KBr, cm^{-1}): 2200 (cyano); 1702 (ester carbonyl); 1516, 1340 (nitro). ^{1}H NMR ($CDCl_3$) ppm: 8.17 (m, 2H, phenylene ortho to nitro); 7.84–7.06 (m, 11H, other phenylene; 1H, cyanovinylene); 2.83 (t, 2H, $CH_2(CH_2)_2COO$); 2.32 (t, 2H, $(CH_2)_2CH_2COO$); 2.02 (m, 2H, $CH_2CH_2CH_2COO$). Anal. Calcd. for $C_{86}H_{20}N_2O_4$: C, 90.20; H, 1.76; N, 2.45. Found: C, 89.63; H, 1.38; N, 2.21.

Characterization Methods: IR spectra were recorded on a Perkin-Elmer 16PC FTIR spectrometer with KBr pellets. ^{1}H NMR (400 MHz) spectra were obtained using a Brucker spectrometer. Chemical shifts (δ values) are given in parts per million with tetramethylsilane as an internal standard. UV–vis spectra were recorded on a Beckman DU-640 spectrometer with spectrograde chloroform. Elemental analyses were carried out with a Carlo Erba model EA1108 analyzer.

The electrochemical properties of PCBM and **F** were studied by cyclic voltammetry (CV) (CH Instruments). A glassy carbon coated with PCBM or **F**, a Pt plate and an Ag/Ag$^+$ electrode were used as the working-, counter- and reference-electrode respectively. The electrolyte solution was 0.1 M tetrabutylammonium hexafluorophosphate (Bu_4NPF_6) in anhydrous acetonitrile. The potential scan rate was 100 mV s^{-1}. The films for the electrochemical measurements were coated from chloroform solutions.

The crystallinity of the films was studied using the X-ray diffraction (XRD) technique (panalytical make USA) having CuKα, as radiation source of wavelength λ = 1.5405 Å with the films coated on the quartz substrates. AFM images were recorded using digital instrument nanoscope in trapping mode.

Device Fabrication and Characterization: The blend solutions of P3HT:PCBM or P3HT:**F** (1:1 w/w) were prepared using chloroform in concentration 10 mg mL^{-1} and stirred for 2 h. For the preparation of mixed solventss, 0.05 mL of acetone was added to 1 mL P3HT:**F** solution in chloroform and then stirred for another 2 h. The PSCs were fabricated according to the following procedure. First, the indium doped tin oxide (ITO) coated glass substrate was cleaned with detergent, then ultrasonicated in distilled water and isopropyl alcohol and finally dried overnight in an oven at 80 °C. To supplement this bottom electrode, a hole transport layer of PEDOT:PSS (BAYTRON, conductive grade) was spin cast from aqueous solution on the ITO coated glass substrate, and was subsequently dried at 80 °C for 20 min. The photoactive layer of the blend (P3HT:PCBM or P3HT:**F**) was deposited by spin coating the prepared blend solutions on the top of the PEDOT:PSS layer. The thickness of the photoactive layer is approximately 80–85 nm. Finally, an aluminium (Al) electrode (thickness about 100 nm) was deposited by thermal evaporation under high vacuum (1×10^{-5} mbar). The effective area of the devices is 10 mm^2. For thermal annealing, the blend films were placed on a hot plate and annealed at temperature of 120 °C for 2 min, before the deposition of Al electrode. The hole only devices, i.e., ITO/PEDOT:PSS/blend/Au, used to extract hole mobility in the blend films, were fabricated as described above, except that the top electrode was replaced with Au (60 nm). Electron only devices having structure Al/blend/Al, were also fabricated by spin coating the active layer on glass/Al substrates, followed by the deposition of Al cathode electrode.

The current–voltage (*J–V*) measurement of the devices was carried out on a computer controlled Keithley 238 source meter. A xenon lamp (500 W) was used as white light source and the optical power at the sample was 100 mW cm^{-2} (the equivalent of one sun at 1.5 AM). The AM 1.5 spectrum was obtained from the light source with the use of air mass 1.5 filter.

Acknowledgements

We are thankful to Prof. Y. K. Vijay of Thin film and Membrane Science Laboratory, University of Rajasthan Jaipur (Raj.) for allowing us to undertake the device fabrication and characterization in his laboratory.

Received: August 31, 2010
Revised: October 8, 2010
Published online: December 13, 2010

[1] (a) G. Yu, J. Gao, J. C. Hummelen, F. Wudl, A. J. Heeger, *Science* **1995**, *270*, 1789; (b) J. J. M. Halls, C. A. Walsh, N. C. Greenham, E. A. Marseglia, R. H. Friend, S. C. Moratti, A. B. Holmes, *Nature* **1995**, *376*, 498; (c) B. C. Thompson, J. M. J. Fréchet, *Angew. Chem. Int. Ed.* **2008**, *47*, 58; (d) S. Günes, H. Neugebauer, N. S. Sariciftci, *Chem. Rev.* **2007**, *107*, 1324; (e) C. J. Brabec, N. S. Sariciftci, J. C. Hummelen, *Adv. Funct. Mater.* **2001**, *11*, 15; (f) K. M. Coakley, M. D. MeGehee, *Chem. Mater.* **2004**, *16*, 4533; (g) Y.-J. Cheng, S.-H. Yang, C.-S. Hsu, *Chem. Rev.* **2009**, *109*, 5868.

[2] (a) M. C. Scharber, D. Mühlbacher, M. Koppe, P. Denk, C. Waldauf, A. J. Heeger, C. J. Brabec, *Adv. Mater.* **2006**, *18*, 789; (b) L. J. A. Koster, V. D. Mihailetchi, P. W. M. Blom, *Appl. Phys. Lett.* **2006**, *88*, 093511.

[3] G. Li, V. Shrotriya, J. S. Huang, Y. Yao, T. Moriarty, K. Emery, Y. Yang, *Nat. Mater.* **2005**, *4*, 864.

[4] W. Ma, C. Yang, X. Gong, K. Lee, A. J. Heeger, *Adv. Funct. Mater.* **2005**, *15*, 1617.

[5] Y. Kim, S. Cook, S. M. Tuladhar, S. A. Choulis, J. Nelson, J. R. Durrant, D. D. C. Bradley, M. Giles, I. MuCulloch, C. S. Ha, M. Ree, *Nat. Mater.* **2006**, *5*, 197.

[6] J. C. B. Hummelen, W. Knight, F. LePeq, F. Wudl, J. Yao, C. L. Wilkins, *J. Org. Chem.*, **1995**, *60*, 532.

[7] J. Peet, J. Y. Kim, N. E. Coates, W. L. Ma, D. Moses, A. J. Heeger, G. C. Bazan, *Nat. Mater.* **2007**, *6*, 497.

[8] C. J. Brabec, A. Cravino, D. Meissner, N. S. Sariciftci, T. Fromherz, M. T. Rispens, L. Sanchez, J. C. Hummelen, *Adv. Funct. Mater.* **2001**, *11*, 374.

[9] J. X. Li, N. Sun, Z. X. Guo, C. J. Li, Y. F. Li, L. M. Dai, D. B. Zhu, D. K. Sun, Y. Cao, L. Z. Fan, *J. Phys. Chem. B* **2002**, *106*, 11509.

[10] L. P. Zheng, Q. M. Zhou, X. Y. Deng, M. Yuang, G. Yu, Y. J. Cao, *J. Phys. Chem. B* **2004**, *108*, 11921.

[11] (a) I. Riedel, N. Martin, F. Giacalone, J. L. Segura, D. Chirvase, J. Parisi, V. Dyakonov, *Thin Solid Films* **2004**, *451*, 43; (b) I. Riedel, E. von Hauff, J. Parisi, N. Martín, F. Giacalone, V. Diakonov, *Adv. Funct. Mater.*, **2005**, *15*, 1979.

[12] S. A. Backer, K. Sivula, D. F. Kavulak, J. M. J. Frechet, *Chem. Mater.* **2007**, *19*, 2927.

[13] F. B. Kooistra, J. Knol, F. Kastenberg, L. M. Popescu, W. J. H. Verhees, J. M. Kroon, J. C. Hummelen, *Org. Lett.* **2007**, *9*, 551.

[14] C. Yang, J. Y. Kim, S. Cho, J. K. Lee, A. J. Heeger, F. Wudl, *J. Am. Chem. Soc.* **2008**, *130*, 644.

[15] J. A. Renz, P. A. Troshin, G. Gobsch, V. F. Razumov, H. Hoppe, *J. Mater. Chem.* **2003**, *13*, 800.

[16] P. A. Troshin, H. Hoppe, J. Renz, M. Egginger, J. Y. Mayorova, A. E. Goryachev, A. S. Peregudov, R. N. Lyubovskaya, G. Gobsch, N. S. Sariciftci, V. F. Razumv, *Adv. Funct. Mater.* **2009**, *19*, 779.

[17] F. B. Kooistra, V. D. Mihailetchi, L. M. Popescu, D. Kronholm, P. W. M. Blom, J. C. Hummelen, *Chem. Mater.* **2006**, *18*, 3068.

[18] J. H. Hou, H. Y. Chen, S. Q. Zhang, G. Li, Y. Yang, *J. Am. Chem. Soc.* **2008**, *130*, 16144.

[19] C.-P. Chen, S.-H. Chan, T.-C. Chao, C. Ting, B.-T. Ko, *J. Am. Chem. Soc.* **2008**, *130*, 12828.

[20] M. M. Wienk, M. Turbiez, J. Gilot, R. A. J. Janssen, *Adv. Mater.* **2008**, *20*, 2556.

[21] Y. Y. Liang, Y. Wu, D. Q. Feng, S.-T. Tsai, H.-J. Son, G. Li, L. P. Yu, *J. Am. Chem. Soc.* **2009**, *131*, 56.

[22] M. M. Wienk, J. M. Kroon, W. J. H. Verhees, J. Knol, J. C. Hummelen, P. A. V. Hal, R. A. J. Janssen, *Angew. Chem. Int. Ed.* **2003**, *42*, 3371.

[23] (a) M. Lenes, G. J. A. H. Wetzelaer, F. B. Kooist, S. C. Veenstra, J. C. Hummelen, P. W. M. Blom, *Adv. Mater.* **2008**, *20*, 2116; (b) M. Lenes, S. W. Shelton, A. B. Sieval, D. F. Kronholm, J. C. Hummelen, P. W. M. Blom, *Adv. Funct. Mater.* **2009**, *19*, 3002.

[24] R. B. Ross, C. M. Cardona, D. M. Guldi, S. G. Sankaranarayanan, M. O. Reese, N. Kopidakis, J. Peet, B. Walker, G. C. Bazan, E. V. Keuren, B. C. Holloway, M. Drees, *Nat. Mater.* **2009**, *8*, 208.

[25] Y. He, H.-Y. Chen, J. Hou, Y. Li, *J. Am. Chem. Soc.* **2010**, *132*, 1377.

[26] G. Zhao, Y. He, Y. Li, *Adv. Mater.* **2010**, 22, 4355.

[27] J. L. Delgado, P.-A. Bouit, S. Filippone, M. Á. Herranza, N. Martín, *Chem. Commun.* **2010**, *46*, 4853.

[28] J. A. Mikroyannidis, D. V. Tsagkournos, P. Balraju, G. D. Sharma, *Org. Electron.* **2010**, *11*, 1242.

[29] Q. Wei, T. Nishizawa, K. Tajima, K. Hashimoto, *Adv. Mater.* **2008**, *20*, 2211.

[30] (a) T. Suzuki, Q. Li, K. C. Khemani, F. Wudl, O. Almarsson, *Science* **1991**, *154*, 1186; (b) M. Prato, T. Suzuki, H. Foroudian, Q. Li, K. Khemani, F. Wudl, *J. Am. Chem. Soc.* **1993**, *115*, 1148.

[31] Y. F. Li, Y. Cao, D. L. Wang, G. Yu, A. J. Heeger, *Synth. Met.* **1999**, *99*, 243.

[32] Q. J. Sun, H. Q. Wang, C. H. Yang, Y. F. Li, *J. Mater. Chem.* **2003**, *13*, 800.

[33] P. J. Brown, D. C. Thomas, A. Kohler, J. S. Wilson, J. S. Kim, C. M. Ramsalale, H. Sirringhaus, R. H. Friend, *Phys. Rev. B—Condens Matter, Mater. Phys.* **2003**, *67*, 064203.

[34] L. G. Li, G. H. Lu, X. He, *J. Mater. Chem.* **2008**, *18*, 1984.

[35] V. D. Mihailetchi, H. Xie, B. de Boer, L. J. A. Koster, P. W. M. Blom, *Adv. Funct. Mater.* **2006**, *16*, 699.

[36] C. J. Brabec, A. Cravino, D. Meissner, N. S. Sariciftci, T. Fromherz, M.T. Rispens, L. Sanchez, J. C. Hummelen, *Adv. Mater.* **2001**, *11*, 374.

[37] J. Jo, S. S. Kim, S. I. Na, B. K. Yu, D. Y. Kim, *Adv. Funct. Mater.* **2009**, *19*, 866.

[38] (a) C. Muller, T. A. M. Ferenczi, M. Campoy-Ouiles, J. M. Frost, D. D. C. Bradley, P. Smith, N. Stingelin-Stutzmann, J. Nelson, *Adv. Mater.* **2008**, *20*, 3510; (b) B. K. Kuila, A. K. Nandi, *J. Phys. Chem. B* **2006**, *110*, 1621.

[39] (a) Y. Zhao, Z. Xie, Y. Qu, Y. Geng, L. Wang, *Appl. Phys. Lett.* **2007**, *90*, 043504; (b) G. Li, Y. Yao, H. Yang, V. Shrotriya, G. Yang, Y. Yang, *Adv. Funct. Mater.* **2007**, *17*, 1636.

[40] S. Berson, R. De Bettignies, S. Bailly, S. Guillerez, *Adv. Funct. Mater.* **2007**, *17*, 1377.

[41] (a) A. J. Moule, K. Meerholz, *Adv. Funct. Mater.* **2008**, *20*, 240; (b) L. Li, G. Lu, X. Yang, *J. Mater. Chem.* **2008**, *18*, 1984; (c) Y. Yao, J. Hou, Z. Xu, G. Li, Y. Yang, *Adv. Funct. Mater.* **2008**, *18*, 1783.

[42] (a) K. Vandewal, A. Gadisa, W. D. Oosterbaan, S. Bertho, F. Banishoeib, I. Van Severen, L. Lutsen, T. J. Cleji, D. Vanderzande, J. V. Manca, *Adv. Funct. Mater.* **2008**, *18*, 2064; (b) J. Cornil, D. Beljonne, J. P. Calbert, J. L. Bredas, *Adv. Mater.* **2001**, *13*, 1053.

[43] M. Brinkmann, J. C. Wittmann, *Adv. Mater.* **2006**, *18*, 860.

[44] (a) D. Gupta, S. Mukhopadhyay, K. S. Narayan, *Sol. Energy Mater. Sol. Cells* **2008**, *94*, 1390; (b) M. H. Yun, G. H. Kim, C. Yang, J. Y. Kim, *J. Mater. Chem.* Doi: 10.1039/c0jm00790k; (c) V. D. Mihailetchi, J. Wildeman, P. W. M. Blom, *Phys. Rev. Lett.* **2005**, *94*, 126602.

[45] (a) A. M. Goodman, A. Rose, *J. Appl. Phys.* **1971**, *42*, 2823; (b) L. J. A. Koster, E. C. P. Smits, V. D. Mihailetchi, P. W. M. Blom, *Phys. Rev. B—Condens Mater. Mater. Phys.* **2005**, *72*, 085205.

[46] (a) X. Yang, J. Loss, S. C. Veenstra, W. J. H. Verhees, M. M. Wienk, J. M. Kroons, M. A. J. Michels, R. A. J. Janssen, *Nano Lett.* **2005**, *5*, 579; (b) J. H. Park, J. S. Kim, J. H. Lee, W. H. Lee, K. Cho, *J. Phys. Chem. C* **2009**, *113*, 17579.